New Journal of Physics

CrossMark

PAPER

Stochastic efficiency: five case studies

Karel Proesmans and Christian Van den Broeck

Hasselt University, B-3590 Diepenbeek, Belgium

E-mail: Karel.proesmans@uhasselt.be

Abstract

Stochastic efficiency is evaluated in five case studies: driven Brownian motion, effusion with a thermo-chemical and thermo-velocity gradient, a quantum dot and a model for information to work conversion. The salient features of stochastic efficiency, including the maximum of the large deviation function at the reversible efficiency, are reproduced. The approach to and extrapolation into the asymptotic time regime are documented.

The concept of Carnot efficiency is a founding principle of macroscopic thermodynamics. It allows to introduce entropy as a state function and to define the Kelvin temperature scale. It states that, for a system operating between two reservoirs at temperatures T_h and T_c, the efficiency $\bar{\eta} = W/Q_h$, being the ratio of output work W over input heat Q_h, is bounded by the Carnot efficiency $\bar{\eta} \leqslant \eta_C$ with $\eta_C = 1 - T_c/T_h$. Right from the start, the question was raised about the efficiency of small scale machines. Maxwell introduced a small-scale demon which was deemed to rectify thermal fluctuations. A clarifying rebuttal was given by Smoluchowski, who proposed a mechanical implementation of the Maxwell demon, the so-called ratchet and pawl. He stressed that this small-scale device would eventually thermalize, after which any rectification would stop. Szilard introduced an information driven engine which seemed to be able to extract work from a single reservoir, in violation with the Carnot prediction. Since he believed that this could not be true, he concluded that there had to be a thermodynamic cost associated to the information gathering [1]. The Szilard engine gave rise to a prolonged scientific discussion about the source of dissipation [2]. It is not the measurement or computational process, but the resetting process of the memory device that seems to be the dissipative step. The Smoluchowski engine was revisited by Feynman, who showed by an explicit model calculation that the efficiency of the ratchet and pawl in contact with two reservoirs is indeed bounded by the Carnot efficiency. A subtle error in his analysis was elucidated by Parrondo and Sekimoto [3, 4], indicating that the efficiency was strictly below Carnot efficiency in this model. This was confirmed by a more detailed analysis on simplified models [5, 6], prompting the question whether Carnot efficiency could at all be reached in such small devices [7]. These questions have led to major interest in information to work conversion, both theoretically [8–18] and experimentally [19–25].

Thermodynamic efficiency can also be defined for other types of engines, notably for work to work and the above mentioned information to work transformations. In the case of a transformation of input work W_i to output work W_o, the thermodynamic efficiency is defined as $\bar{\eta} = W_o/W_i$. The analogue of Carnot efficiency is reached for a reversible operation leading to $W_o = W_i$ (since no heat is dissipated). Hence the second law stipulates $\bar{\eta} \leqslant \eta_r$, with the reversible efficiency is $\eta_r = 1$. For information to work transformation, we note that information about the system can be used to extract work. The reversible limit has been known since the work of Szilard, namely $k_B T \ln 2$ of work can be extracted per bit of information (in an environment operating at temperature T). One bit corresponds to a Shannon information of $I = \ln 2$. More generally, in a transformation of a Shannon information amount I into an amount W of work, the efficiency $\bar{\eta} = W/(k_B T I)$ is upper bounded by the reversible result $\eta_r = 1$.

Over the past two decades, one has been able to reformulate thermodynamics to describe fluctuating small-scale systems. The most notable of the results is the fluctuation theorem, stating that the probability for a stochastic entropy production $\Delta_i s$ is exponentially more probable than that of a corresponding decrease $-\Delta_i s$ in an 'inverse' experiment:

$$\frac{P(\Delta_i s)}{\tilde{P}(-\Delta_i s)} = \exp(k_B \Delta_i s). \tag{1}$$

The tilde refers to the 'time- inverse' experiment. The above symmetry relation for the probability implies the following integral fluctuation theorem:

$$\langle \exp(-k_B \Delta_i s) \rangle = 1, \tag{2}$$

which in term implies the 'second law':

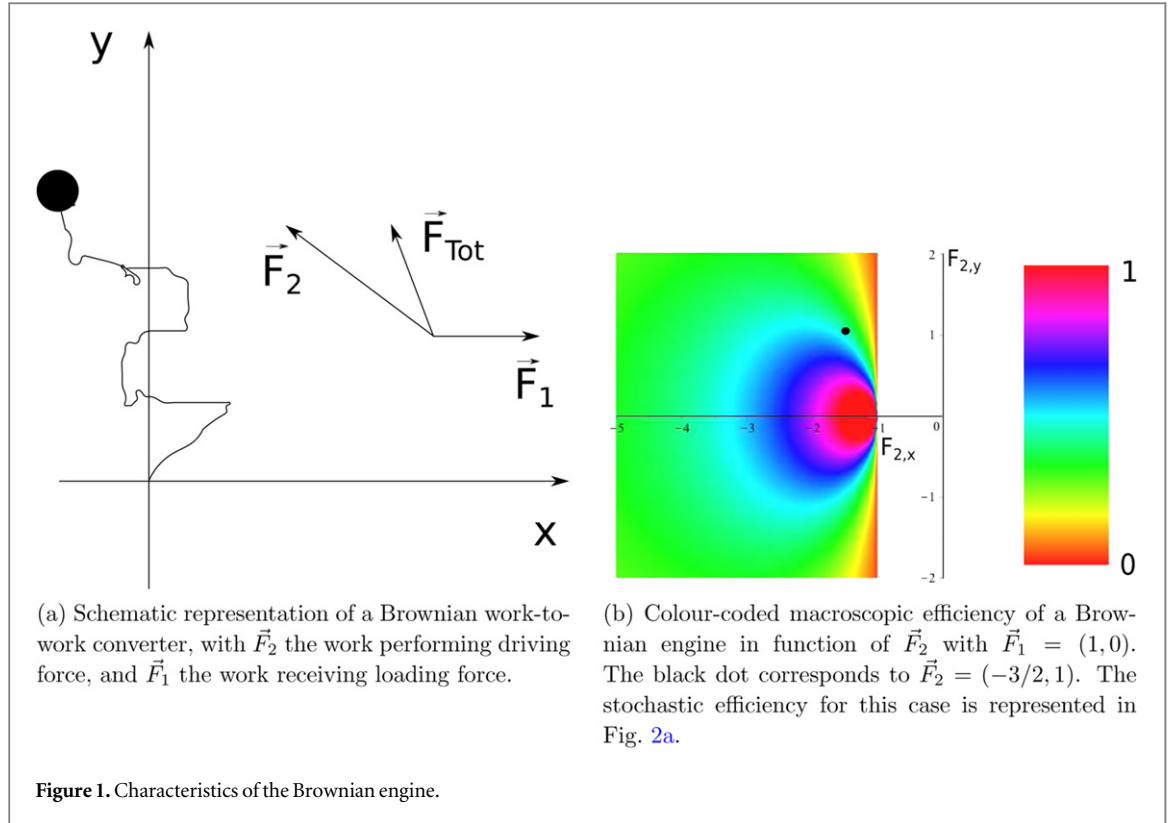$$\langle \Delta_i s \rangle \geqslant 0. \tag{3}$$

The detailed and integral fluctuation theorems (1) and (2) have been derived in many different settings, see for example the Jarzynski [26] and Crooks [27] equalities, and stochastic thermodynamics [28, 29]. When considering a finite time experiment, the interpretation of (1) is somewhat delicate, and there may be restrictions, for example on the initial and final states of the experiment, cf [30] for a recent discussion. The fluctuation theorem however appears to have a wide ranging validity, comparable to the second law, when considering the asymptotic long time limit, in which case (1) reduces to a statement about the large deviation properties of the entropy production. The theorem was actually first derived in this context [31–34]. Surprisingly, the impact of these new insights on the efficiency, and in particular on its stochastic properties, has only been considered very recently [35–43], and only in work to work and heat to work converters. When running a small-scale engine for a finite time, the corresponding cumulated work output and heat uptake, w and q_h, or work output w_o and work input w_i, are stochastic quantities, and hence so is the corresponding stochastic efficiency $\eta = w/q_h$ or $\eta = w_o/w_i$. Starting with the detailed fluctuation theorem (1), it was pointed out that one can make universal statements about the stochastic efficiency η, as it approaches the macroscopic efficiency. More precisely, for large but finite times, values of the stochastic efficiency η different from the macroscopic efficiency $\bar{\eta}$ are exponentially unlikely, as described by the large deviation function $J(\eta) = -\lim_{t \to \infty} 1/t \ln P_t(\eta)$, $J(\eta) \geqslant J(\bar{\eta}) = 0$. For the case of a thermodynamic machine driven by a time-symmetric protocol, it was shown that the reversible efficiency is the least likely, i.e., the large deviation function $J(\eta)$ has a maximum at $\eta = \eta_r$. The macroscopic efficiency is reproduced as the value carrying all probability to dominant order $J(\bar{\eta}) = 0$. For time-asymmetric protocols, the large deviation curves of the stochastic efficiency for the forward and backward experiment cross at the reversible efficiency [36, 37].

In this paper, we provide an explicit and comprehensive illustration of the stochastic efficiency in five engines under a time-symmetric protocol. Providing possibly the simplest steady state models for work to work and heat to work transformation, we consider a Brownian particle subject to competing forces [35] and effusion between two compartments [38]. Even though these cases have been discussed in some detail in the literature, they are introduced briefly for completeness and for comparison with the other models. The third model is a thermal engine based on a quantum dot. It is of interest because its stochastic thermodynamic properties have been discussed and measured, and because it is in principle richer than the effusion model, which can be recovered in an appropriate mathematical limit. In the last two problems, we evaluate stochastic efficiency in novel settings. We show that the universal features of stochastic efficiency are valid for energy to momentum transformation. This is illustrated on an effusion model with momentum transfer. Finally, we discuss the stochastic efficiency for information to work transformation. It is indeed possible to reformulate the fluctuation theorem when dealing with an information processing set-up, such as the one introduced by Szilard. In particular one can introduce the stochastic efficiency $\eta = w/i$ for a machine transforming a stochastic amount of input (Shannon) information i into work w. We show that its large deviation function again displays the same general features. In particular, the reversible efficiency $\eta_r = 1$ is exponentially less likely than any other efficiency in the asymptotic time limit (for time-symmetric protocols). We illustrate these features on the Mandal–Jarzynski model [8, 10].

1. Brownian engine

Consider an overdamped Brownian particle on a plane, subject to two external forces, a loading force $\vec{F}_1$, and a driving force $\vec{F}_2$ [35], cf figure 1(a). The (larger) driving force $\vec{F}_2$ pushes the particle against the loading force $\vec{F}_1$. The stochastic efficiency of such a device as a work-to-work converter was discussed in [35, 39]. The mathematics are very simple. Considering for simplicity a two-dimensional set-up, the displacement $\vec{x}$ of the Brownian particle during a time t is characterized by a two-dimensional Gaussian distribution. Under influence of the resulting force $\vec{F} = \vec{F}_1 + \vec{F}_2$ the average displacement is $\langle \vec{x} \rangle = \mu \vec{F} t$, μ being the mobility. The variance is isotropic and uncorrelated in orthogonal directions, $\langle \delta \vec{x} \delta \vec{x} \rangle = 2Dt \vec{1}$, where D is the diffusion coefficient and $\vec{1}$ the unit matrix.

We first turn to the macroscopic efficiency, which is very easy to evaluate, see also figure 1(b) for a colour-coded illustration:

(a) Schematic representation of a Brownian work-to-work converter, with $\vec{F}_2$ the work performing driving force, and $\vec{F}_1$ the work receiving loading force.

(b) Colour-coded macroscopic efficiency of a Brownian engine in function of $\vec{F}_2$ with $\vec{F}_1 = (1, 0)$. The black dot corresponds to $\vec{F}_2 = (-3/2, 1)$. The stochastic efficiency for this case is represented in Fig. 2a.

Figure 1. Characteristics of the Brownian engine.

$$\bar{\eta} = -\frac{\langle w_1 \rangle}{\langle w_2 \rangle} = -\frac{\vec{F}_1 \cdot \langle \vec{x} \rangle}{\vec{F}_2 \cdot \langle \vec{x} \rangle} = -\frac{\vec{F}_1 \cdot \vec{F}}{\vec{F}_2 \cdot \vec{F}}, \tag{4}$$

where $w_1 = \vec{F}_1 \cdot \vec{x}$ and $w_2 = \vec{F}_2 \cdot \vec{x}$ are the stochastic amounts of work delivered by the loading and driving force respectively. The engine regime, i.e., the regime where the driving force delivers a positive amount of work to the loading force, is determined by:

$$-\frac{\left|\vec{F}_2\right|}{\left|\vec{F}_1\right|} \leqslant \cos\theta \leqslant -\frac{\left|\vec{F}_1\right|}{\left|\vec{F}_2\right|}, \tag{5}$$

with θ is the angle between $\vec{F}_1$ and $\vec{F}_2$. In combination with (4), it is clear from (5) that, in the engine regime, the macroscopic efficiency is bounded by $\bar{\eta} \leqslant \eta_r = 1$. The reversible efficiency $\eta_r = 1$ can only be reached in the limit $\vec{F}_2 \rightarrow -\vec{F}_1$ while $\vec{F} \not\parallel \vec{F}_1$. This can also be seen in figure 1(b).

We next investigate the stochastic efficiency

$$\eta = -w_1/w_2 = -\vec{F}_1 \cdot \vec{x} / \vec{F}_2 \cdot \vec{x}. \tag{6}$$

Being the ratio of two correlated Gaussian variables, its probability distribution can be evaluated analytically, see also [39]:

$$P_t(\eta) = \frac{\left|\vec{F}_1 \times \vec{F}_2\right| e^{-\frac{t}{t_0}}}{\pi \left(\vec{F}_1 + \eta\vec{F}_2\right)^2} \left(1 + \sqrt{\pi g(\eta)} \, \mathrm{Erf}\left[\sqrt{g(\eta)}\right] e^{g(\eta)}\right), \tag{7}$$

with

$$g(\eta) = \frac{t}{t_0} \frac{(1-\eta)^2 \left(\vec{F}_1 \times \vec{F}_2\right)^2}{\vec{F}^2 \left(\vec{F}_1 + \eta\vec{F}_2\right)^2}, \tag{8}$$

and $\mathrm{Erf}(x)$ is the error function. The characteristic time $t_0 = 2D/(\mu|\vec{F}|)^2$ determines the boundary between diffusion dominated ($t \ll t_0$) and drift dominated ($t \gg t_0$) dynamics. We note in passing that it is easy to show from equations (7) and (8) that $P_t'(0) > 0$ and $P_t'(1) < 0$, implying that there exists at least one maximum in the interval $\eta \in [0, 1]$. This can indeed be seen in the simulation results for $t/t_0 = 2$, 5 and 10, shown in figure 2(a).

(a) Probability distribution $P_t(\eta)$ of the efficiency η for the Brownian engine.

(b) Approach of $-\ln P_t(\eta)/t$ for increasing values of t/t_0 (blue, red and green curve) to the large deviation function $J(\eta)$ (black curve). The purple curve is obtained by extrapolation from the finite time results. The black curve is given by equation (9).

Figure 2. Efficiency fluctuations of a Brownian engine with $\vec{F}_1 = (1, 0)$, $\vec{F}_2 = (-3/2, 1)$ and $\bar{\eta} = 0.29$.

Universal features of the efficiency fluctuations are revealed when studying the asymptotic time behavior via the large deviation function of η [35]:

$$J(\eta) = -\lim_{t \to \infty} \frac{1}{t} \ln P_t(\eta)$$

$$= \frac{\mu^2}{4D} \frac{\left[(\vec{F}_1 + \eta \vec{F}_2) \cdot (\vec{F}_1 + \vec{F}_2) \right]^2}{(\vec{F}_1 + \eta \vec{F}_2)^2}. \tag{9}$$
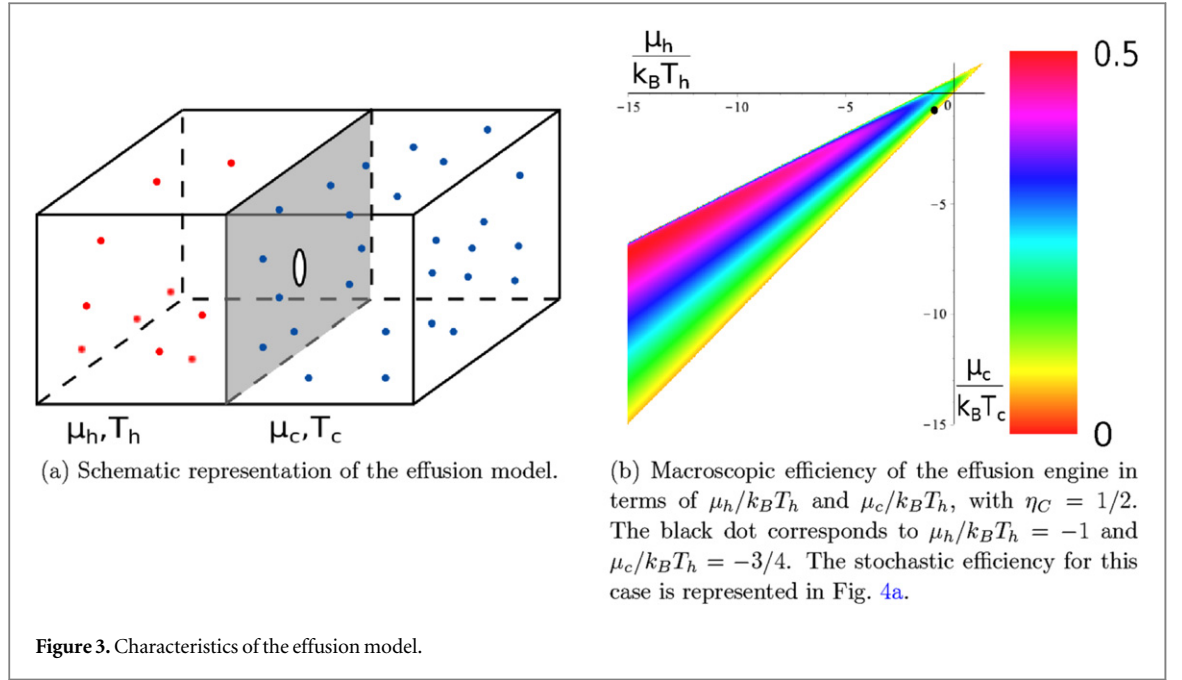
This function has a minimum at the macroscopic efficiency $J(\bar{\eta}) = 0$, but also a maximum at the reversible efficiency $\eta_r = 1$, with equal asymptotes in the limits $\eta \to \pm\infty$. To illustrate the approach to the large deviation regime, $-\ln(P_t(\eta))/t$ is plotted in figure 2(b) obtained from simulation results for $t/t_0 = 2$, 5, and 10, together with the limiting expression (9). We also include the result of an extrapolation ansatz [38], described in more detail in appendix A. The extrapolation, based on the $t/t_0 = 2$, 5, and 10 curves, is in surprisingly good agreement with the exact asymptotic expression. Although these finite time results do not, in this particular instance, exhibit a maximum close to the reversible efficiency $\eta_r = 1$, it does show up by extrapolation.

2. Effusion engine

The effusion engine [38] consists of two reservoirs, exchanging heat and particles by effusion via one or more small holes in the separating wall, cf figure 3(a). The reservoirs are supposed to be infinitely large and at equilibrium. The holes are smaller than the mean free path so that the equilibrium state is not disturbed by the effusion process. In this set-up, the flux out of a reservoir is determined by the driving parameter $\mu/(k_B T)$. Under proper working conditions, a net flux of particles moves from say the left compartment, at high temperature T_h and low chemical potential μ_h, to the right compartment at lower temperature T_c but higher chemical potential μ_c.

When a particle moves from the hot to the cold reservoir, it delivers an amount of work $w_0 = \mu_c - \mu_h = \Delta\mu$, while extracting an amount of heat $q_0 = u_0 - \mu_h$ from the hot reservoir, where u_0 is the kinetic energy of the transferred particle. Therefore, after a net transfer of n particles, the total amount of delivered work and extracted heat, w and q are given by:

$$w = n\Delta\mu, \tag{10}$$

(a) Schematic representation of the effusion model.

(b) Macroscopic efficiency of the effusion engine in terms of $\mu_h/k_B T_h$ and $\mu_c/k_B T_h$, with $\eta_C = 1/2$. The black dot corresponds to $\mu_h/k_B T_h = -1$ and $\mu_c/k_B T_h = -3/4$. The stochastic efficiency for this case is represented in Fig. 4a.

Figure 3. Characteristics of the effusion model.

$$q = u - n\mu_h, \tag{11}$$

with u the net energy transfer.

Particles with kinetic energy E transfer from the hot to the cold reservoir at rate [44]:

$$T_{h\to c}(E) = \frac{1}{t_0} \frac{E}{\left(k_B T_h\right)^2} e^{-\frac{E}{k_B T_h}}, \tag{12}$$

and from the cold to the hot reservoir at rate

$$T_{c\to h}(E) = \frac{1}{t_0} \frac{E}{\left(k_B T_h\right)^2} e^{-\frac{E}{k_B T_c} + \frac{\mu_c}{k_B T_c} - \frac{\mu_h}{k_B T_h}}, \tag{13}$$

where $t_0 = \sqrt{2\pi m / \left(\sigma^2 \rho_h^2 k_B T_h\right)}$ is the average time between particle crossings from the hot to the cold reservoir, σ is the surface area of the effusion hole and m is the mass of the particles of the gas. The macroscopic efficiency can be easily obtained:

$$
\begin{aligned}
\bar{\eta} &= \frac{\langle w \rangle}{\langle q \rangle} \\
&= \frac{\Delta\mu \langle n \rangle}{\langle u \rangle - \mu_h \langle n \rangle} \\
&= \frac{\Delta\mu \left((k_B T_h)^2 e^{\frac{\mu_h}{k_B T_h}} - (k_B T_c)^2 e^{\frac{\mu_c}{k_B T_c}} \right)}{(k_B T_h)^2 \left(2k_B T_h - \mu_h \right) e^{\frac{\mu_h}{k_B T_h}} - (k_B T_c)^2 \left(2k_B T_c - \mu_h \right) e^{\frac{\mu_c}{k_B T_c}}}.
\end{aligned}
\tag{14}
$$
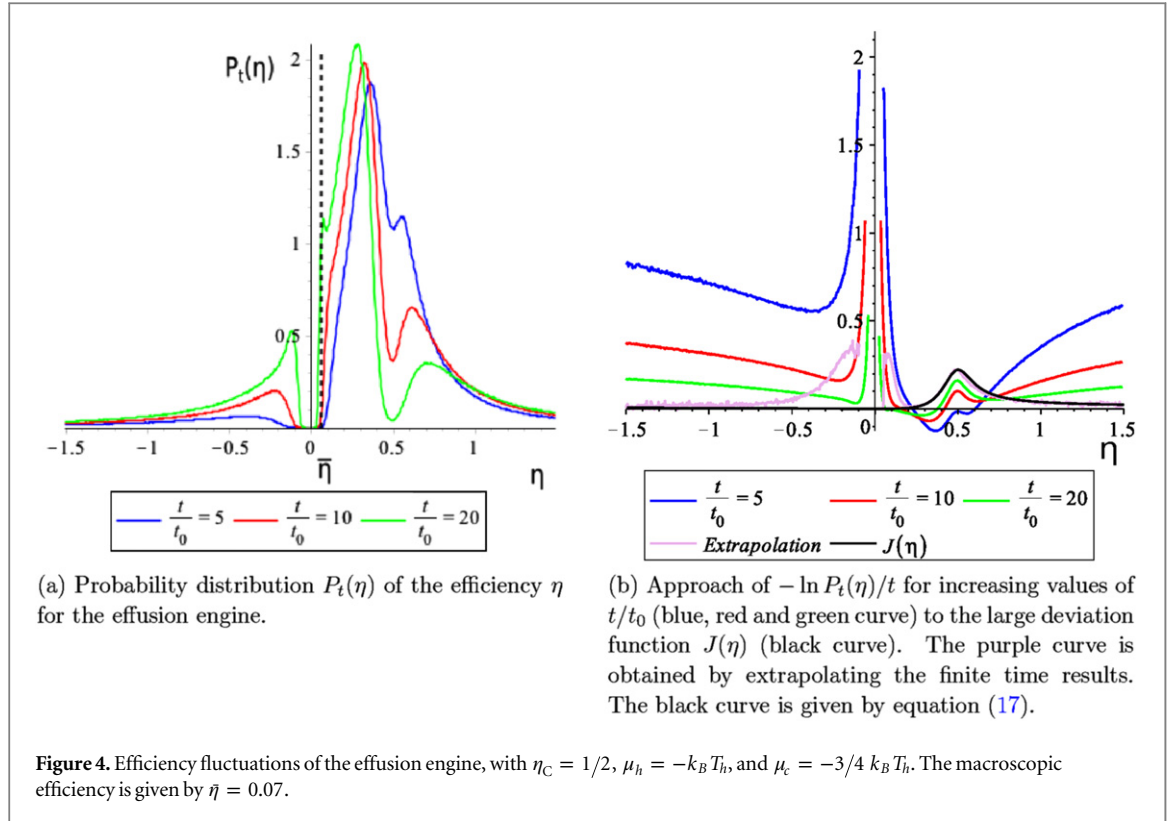
This function is plotted for Carnot efficiency $\eta_C = 1/2$ in figure 3(b) in terms of $\mu_c/k_B T_h$ and $\mu_h/k_B T_h$. The engine boundaries are given by $\mu_h < \mu_c < \mu_h T_c/T_h - 2k_B T_c \ln(T_c/T_h)$. Furthermore, the macroscopic efficiency is bounded by the Carnot efficiency, and this boundary is only reached in the limit $\mu_c, \mu_h \to -\infty$, which, for an ideal gas, corresponds to zero density.

We next investigate the stochastic efficiency

$$\eta = w/q. \tag{15}$$

Since it is not possible to obtain the analytic expression of the probability distribution $P_t(\eta)$, we present results from a numerical simulation of the Markov process with the prescribed rates (12) and (13), cf figure 4(a). For the parameter values under consideration, one clearly sees a minimum in the probability distribution developing in the vicinity of the Carnot efficiency η_C, even at the rather short times represented here. The behavior around $\eta = 0$, and in particular the other minimum around $\eta = 0$, can be explained by the low number of particle crossings for short times [38]: due to the fact that only a few particles will cross, small, non-zero efficiencies can

(a) Probability distribution $P_t(\eta)$ of the efficiency η for the effusion engine.

(b) Approach of $-\ln P_t(\eta)/t$ for increasing values of t/t_0 (blue, red and green curve) to the large deviation function $J(\eta)$ (black curve). The purple curve is obtained by extrapolating the finite time results. The black curve is given by equation (17).

Figure 4. Efficiency fluctuations of the effusion engine, with $\eta_C = 1/2$, $\mu_h = -k_B T_h$, and $\mu_c = -3/4\, k_B T_h$. The macroscopic efficiency is given by $\bar{\eta} = 0.07$.

only be reached if particles cross with very high energies. As this is very unlikely, the finite time probability distribution function shows a minimum around zero.

Turning finally to the asymptotic time behaviour, we note that the large deviation function $J(\eta)$ of the stochastic efficiency can be obtained from the joint cumulant generating function of work and heat $\varphi(\lambda, \omega)$, see [37]. The latter is explicitly known for effusion [44]:

$$\varphi(\lambda, \omega) = \lim_{t \to \infty} \frac{1}{t} \ln \left\langle e^{-\lambda w - \omega q} \right\rangle$$

$$= -\frac{\sigma \rho_h \sqrt{k_B T_h}}{\sqrt{2\pi m}} \left(1 - \frac{\exp\left(-\lambda \Delta \mu - \omega \mu_h\right)}{(1 - k_B T_h \omega)^2} \right)$$

$$- \frac{\sigma \rho_c \sqrt{k_B T_c}}{\sqrt{2\pi m}} \left(1 - \frac{\exp\left(\lambda \Delta \mu + \omega \mu_c\right)}{(1 + k_B T_c \omega)^2} \right). \tag{16}$$

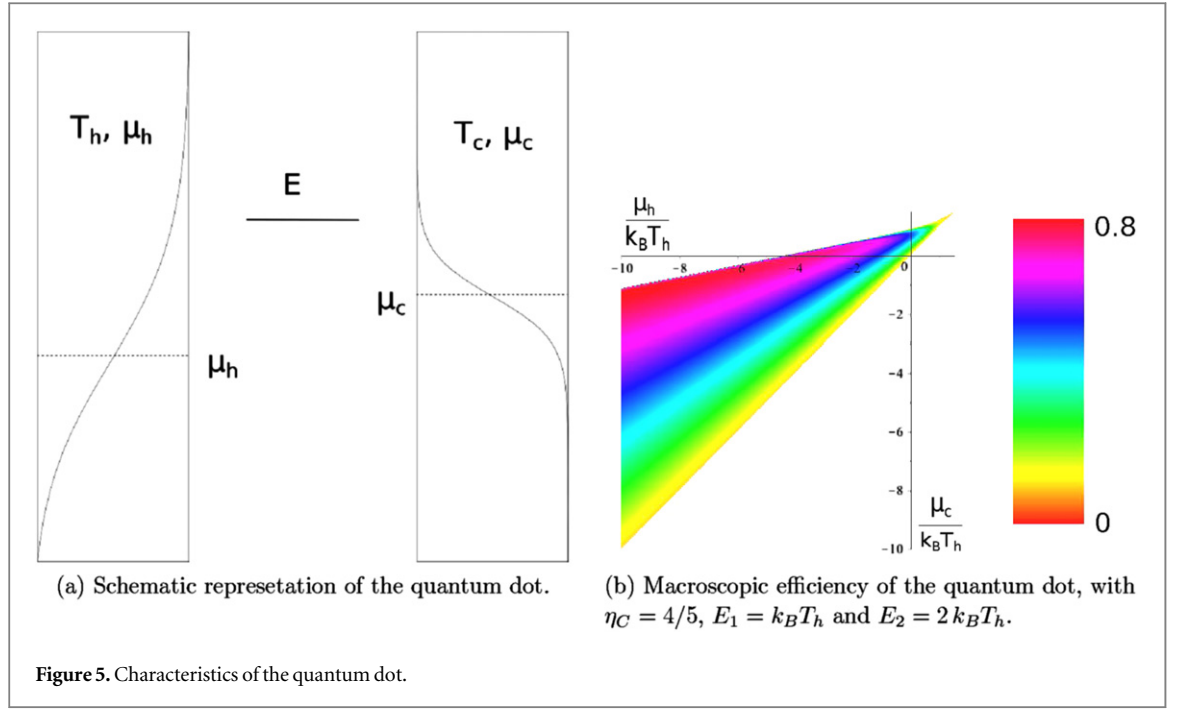The large deviation function of the stochastic efficiency is then given by:

$$J(\eta) = -\min_\lambda \varphi(\lambda, \lambda \eta). \tag{17}$$

The contraction can be done numerically, and the comparison with finite-time simulations is represented in figure 4(b). Note that the extrapolation again works quite well, except in the vicinity of $\eta = 0$, due to the aforementioned short time effects.

3. Quantum dot

The quantum dot model, schematically represented in figure 5(a), has been investigated in detail in the context of stochastic thermodynamics [45–48]. Two electron reservoirs are brought in contact with each other via one or multiple quantum dots. In order to investigate its stochastic efficiency, we focus on the case of two quantum dots, each with one 'active' energy level, E_1 and E_2 ($E_1 < E_2$). We need to consider at least two quantum dots since otherwise the engine is tightly coupled, i.e. the stochastic efficiency will not fluctuate. Occupancy of a quantum dot by multiple electrons is forbidden because of Coulomb repulsion. For mathematical simplicity, we also set all coupling constants between dot and reservoirs equal to Γ.

The operation of each quantum dot as a thermal engine is similar to that of the effusion engine: a net motion of electrons from a reservoir with low chemical potential to one with higher chemical potential is induced by a

(a) Schematic represetation of the quantum dot.

(b) Macroscopic efficiency of the quantum dot, with $\eta_C = 4/5$, $E_1 = k_B T_h$ and $E_2 = 2\,k_B T_h$.

Figure 5. Characteristics of the quantum dot.

driving temperature gradient. For every particle transferring through the quantum dot with the lower energy level E_1, the heat taken from the hot reservoir is given by $\delta q_1 = E_1 - \mu_h$ and the delivered amount of work is $w_0 = \mu_c - \mu_h = \Delta\mu$. Furthermore, the rate of transfer between the hot reservoir and the quantum dot are given by:

$$k_h^+ = \frac{\Gamma e^{-\frac{E_1-\mu_h}{T_h}}}{1 + e^{-\frac{E_1-\mu_h}{T_h}}}, \tag{18}$$

$$k_h^- = \frac{\Gamma}{1 + e^{-\frac{E_1-\mu_h}{T_h}}}. \tag{19}$$

The rate of exchange between the cold reservoir and the quantum dot is obtained by replacing with T_h and μ_h by T_c and μ_c, respectively. Analogous expressions hold for transfer through the other quantum dot, with E_1 replaced by E_2. The total amount of delivered work w and consumed heat q after a net transfer of n_1 particles through the quantum dot with energy level E_1 and n_2 particles through the quantum dot with energy level E_2 are then given by:

$$w = \Delta\mu\left(n_1 + n_2\right), \tag{20}$$

$$q = \delta q_1 n_1 + \delta q_2 n_2. \tag{21}$$

The macroscopic efficiency can now be written as:

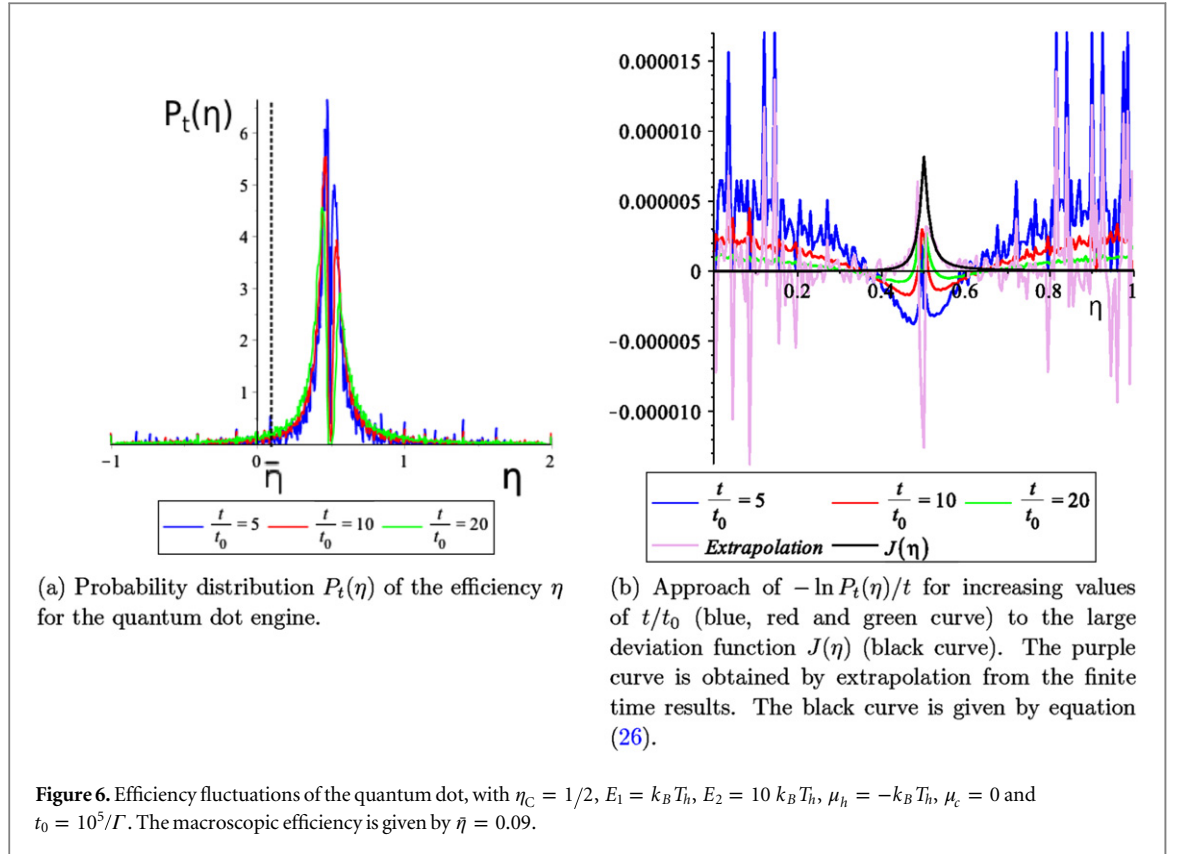$$\bar{\eta} = \frac{\langle w \rangle}{\langle q \rangle} \tag{22}$$

$$= \frac{\Delta\mu\left(\langle n_1 \rangle + \langle n_2 \rangle\right)}{\langle n_1 \rangle\left(E_1 - \mu_c\right) + \langle n_2 \rangle\left(E_2 - \mu_c\right)}, \tag{23}$$

where n_1 and n_2 are the (stochastic) net amount of particles transferred through respectively the quantum dot with the lower and higher energy level. Their average value can be calculated from the rates given in equations (18) and (19):

$$\langle n_1 \rangle = \frac{\Gamma}{2} \frac{e^{\frac{E_1-\mu_c}{T_c}} - e^{\frac{E_1-\mu_h}{T_h}}}{\left(e^{\frac{E_1-\mu_c}{T_c}} + 1\right)\left(e^{\frac{E_1-\mu_h}{T_h}} + 1\right)}, \tag{24}$$

and an analogous expression for $\langle n_2 \rangle$ with E_1 replaced by E_2. The macroscopic efficiency of the engine is plotted in figure 5(b) in function of $\mu_h/k_B T_h$ and $\mu_c/k_B T_h$. These results are comparable with the results of the effusion engine. Again, Carnot efficiency is only reached in the limit of zero density.

(a) Probability distribution $P_t(\eta)$ of the efficiency η for the quantum dot engine.

(b) Approach of $-\ln P_t(\eta)/t$ for increasing values of t/t_0 (blue, red and green curve) to the large deviation function $J(\eta)$ (black curve). The purple curve is obtained by extrapolation from the finite time results. The black curve is given by equation (26).

Figure 6. Efficiency fluctuations of the quantum dot, with $\eta_C = 1/2$, $E_1 = k_B T_h$, $E_2 = 10\, k_B T_h$, $\mu_h = -k_B T_h$, $\mu_c = 0$ and $t_0 = 10^5/\Gamma$. The macroscopic efficiency is given by $\bar{\eta} = 0.09$.

For the study of the efficiency fluctuations at finite time, we again first turn to numerical simulations. The probability distribution $P_t(\eta)$, with

$$\eta = \frac{w}{q}, \tag{25}$$

is obtained by sampling the net fluxes n_1 and n_2 using the rates specified in equations (18) and (19). A typical result is shown in figure 6(a). The results appear to be rather noisy, which is due to the fact that both work and heat, and therefore the efficiency, are discrete variables. Nevertheless, the minimum at Carnot efficiency is very striking, even at these short times. The convergence to the macroscopic efficiency on the other hand is rather slow, which is, in this particular case, due to the small value of the large deviation function.
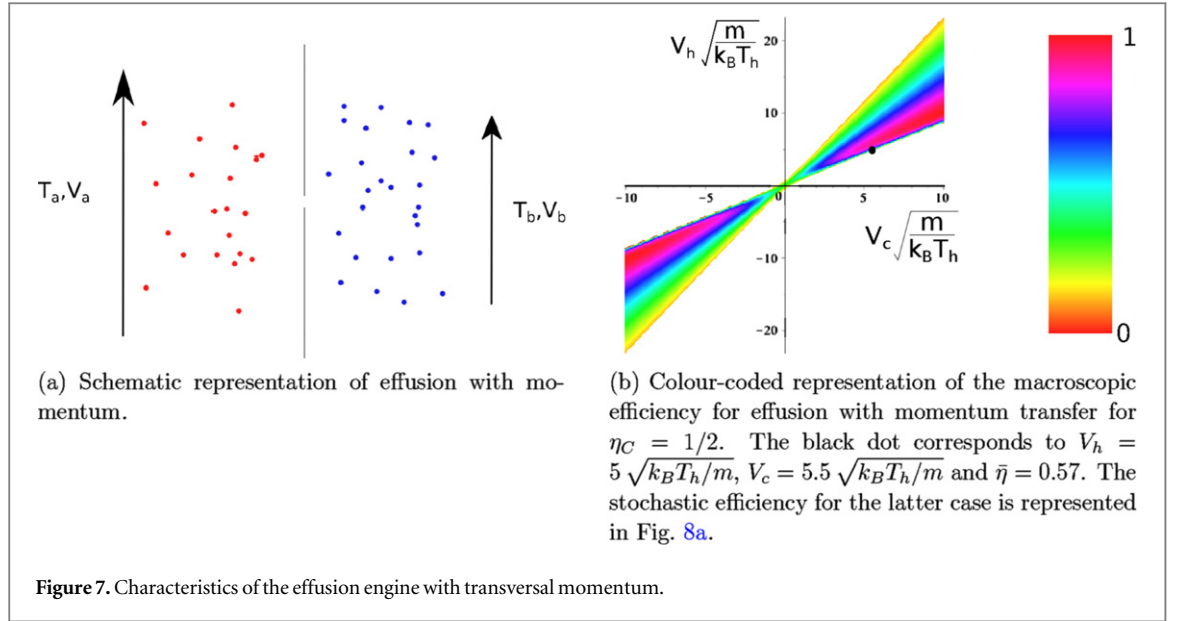
Due to the fact that this engine is driven by two independent, tight-coupled operating channels (namely the two quantum dots), with heat consumption and efficiencies per particle δq_i and $\eta_i = w_0/\delta q_i$ respectively, $i = 1, 2$, the large deviation function for the efficiency $J(\eta)$ can be written in terms of the event large deviation functions $\phi_i(n)$, $i = 1, 2$ (see appendix B):

$$J(\eta) = \min_x \left(\phi_1\left(\frac{\alpha x}{\delta q_1}\right) + \phi_2\left(\frac{(1-\alpha)x}{\delta q_2}\right) \right). \tag{26}$$

Here, $\alpha = (\eta - \eta_2)/(\eta_1 - \eta_2)$, and $\phi_1(n)$ and $\phi_2(n)$ are the large deviation functions of the net number of transferred particles through each of the channels. As these large deviation functions are known (see appendix C), equation (26) allows to estimate the large deviation function of η with great precision. The comparison with finite time numerical simulations is shown in figure 6(b). Note that the extrapolation from finite time results does not work uniformly well due to the aforementioned discreteness of the efficiency.

4. Effusion with momentum transfer

The effusion model, discussed in section 2, has also been studied in the presence of momentum exchange between the reservoirs [49], see figure 7(a). In this set-up, the gases move with overall average speed V_h and V_c parallel to the separating wall containing the effusion hole. For the purpose of illustration, we assume equal densities and chemical potentials in both reservoirs, and consider a thermal engine, with temperatures T_h and T_c in the respective compartments, driving momentum exchange.

(a) Schematic representation of effusion with momentum.

(b) Colour-coded representation of the macroscopic efficiency for effusion with momentum transfer for $\eta_C = 1/2$. The black dot corresponds to $V_h = 5\sqrt{k_B T_h/m}$, $V_c = 5.5\sqrt{k_B T_h/m}$ and $\bar{\eta} = 0.57$. The stochastic efficiency for the latter case is represented in Fig. 8a.

Figure 7. Characteristics of the effusion engine with transversal momentum.

The definition of the efficiency is based on the identification of the additive contributions to the entropy production. For a reversible process, their algebraic sum becomes zero and the resulting macroscopic efficiency (being the negative ratio of the constitutive parts) is equal to 1. In the present case there are three contributions related to energy, particle and momentum exchanges, hence there is some freedom to specify which contribution operates as input, contributing (on average) to a a positive entropy production, and which one is the output generating a negative contribution. We focus here on the thermal engine regime, with the energy flux as input:

$$\eta = -\frac{A_N n + A_{p_x} p_x}{A_U u},\tag{27}$$

with

$$A_N = \frac{3}{2}k_B \ln\left(\frac{T_c}{T_h}\right) + \left(\frac{mV_c^2}{2T_c} - \frac{mV_h^2}{2T_h}\right),\tag{28}$$

$$A_{p_x} = \frac{V_h}{T_h} - \frac{V_c}{T_c},\tag{29}$$

$$A_U = \frac{1}{T_c} - \frac{1}{T_h},\tag{30}$$

the affinities of the particle, momentum and energy transport, and n, p_x and u the amounts of particle, momentum and energy transport. The macroscopic efficiency then reads:
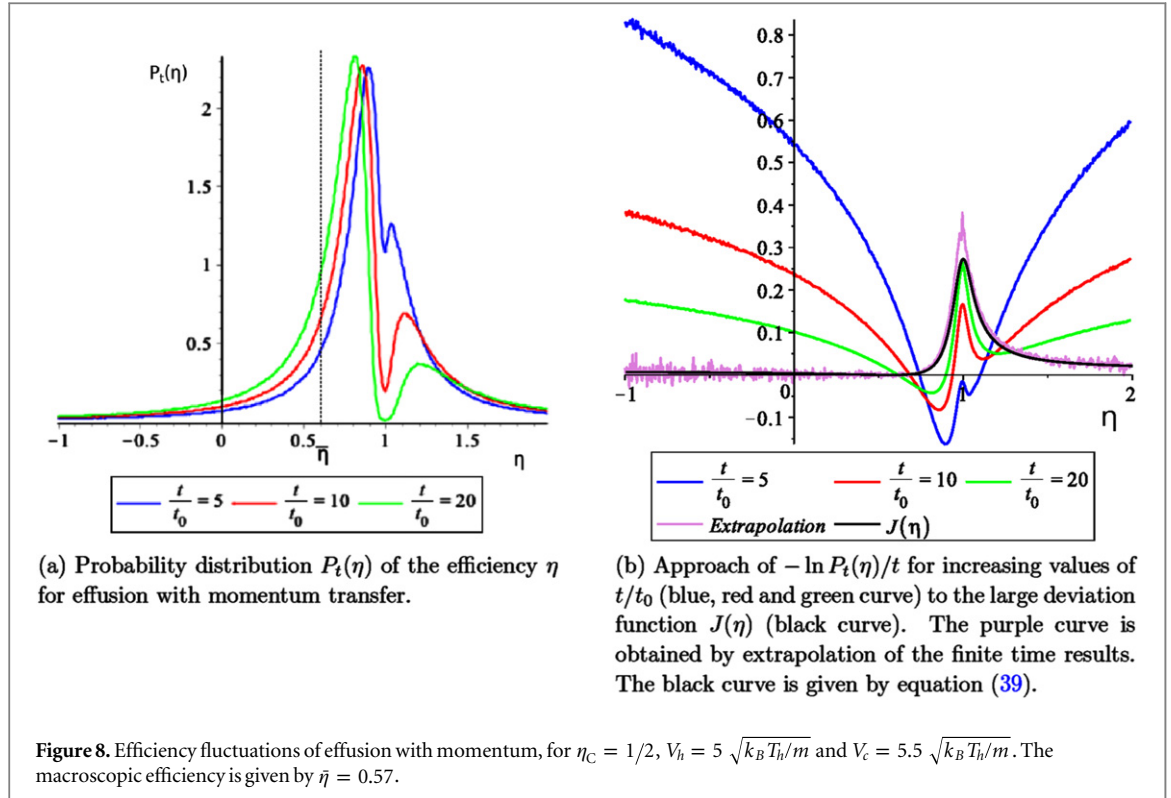
$$\bar{\eta} = -\frac{A_N \langle n \rangle + A_{p_x} \langle p_x \rangle}{A_U \langle u \rangle},\tag{31}$$

with $\langle n \rangle$, $\langle p_x \rangle$ and $\langle u \rangle$, the macroscopic particle, energy and momentum fluxes. The total entropy production is given by [49]:

$$\Delta_i S = A_N \langle n \rangle + A_{p_x} \langle p_x \rangle + A_U \langle u \rangle \geqslant 0.\tag{32}$$

Hence the second law of thermodynamics dictates that macroscopic efficiency in the engine regime is smaller than 1. This is illustrated for the parameter values considered in figure 7(b).

Following the discussion of the previous examples, we now turn to the efficiency fluctuations. For the finite-time probability distribution $P_t(\eta)$, we again rely on numerical simulations. The rates of particle transfer are given by:

(a) Probability distribution $P_t(\eta)$ of the efficiency η for effusion with momentum transfer.

(b) Approach of $-\ln P_t(\eta)/t$ for increasing values of t/t_0 (blue, red and green curve) to the large deviation function $J(\eta)$ (black curve). The purple curve is obtained by extrapolation of the finite time results. The black curve is given by equation (39).

Figure 8. Efficiency fluctuations of effusion with momentum, for $\eta_C = 1/2$, $V_h = 5\sqrt{k_B T_h/m}$ and $V_c = 5.5\sqrt{k_B T_h/m}$. The macroscopic efficiency is given by $\bar{\eta} = 0.57$.

$$
T_{h\to c}\left(E, p_x\right) = \frac{1}{t_0} \frac{\sqrt{2}}{\left(k_B T_h\right)^2 \pi \sqrt{m}} \left(E - \frac{p_x^2}{2m}\right)^{1/2}
$$

$$
\times \exp\left(-\frac{m}{2 k_B T_h}\left(\frac{2\left(E - \frac{p_x^2}{2m}\right)}{m} + \left(\frac{p_x}{m} + V_h\right)^2\right)\right), \tag{33}
$$

$$
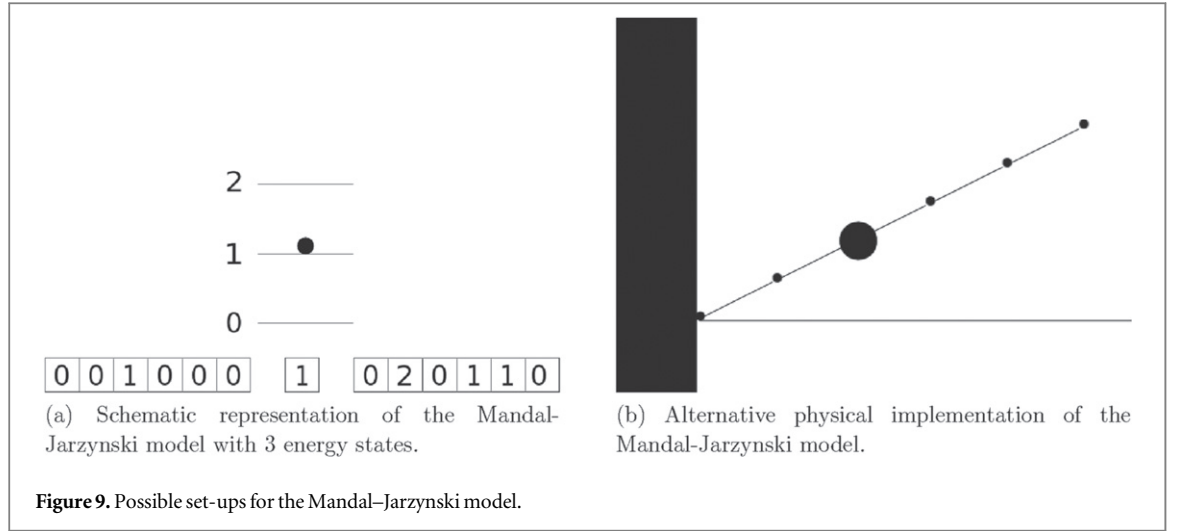T_{c\to h}\left(E, p_x\right) = \frac{1}{t_0} \frac{\sqrt{2}}{\left(k_B T_c\right)^{3/2}\left(k_B T_h\right)^{1/2} \pi \sqrt{m}} \left(E - \frac{p_x^2}{2m}\right)^{1/2}
$$

$$
\times \exp\left(-\frac{m}{2 k_B T_c}\left(\frac{2\left(E - \frac{p_x^2}{2m}\right)}{m} + \left(\frac{p_x}{m} + V_c\right)^2\right)\right), \tag{34}
$$

with $t_0 = \sqrt{2\pi m/(k_B T_h \sigma^2 \rho^2)}$, the average time between particle crossings from reservoir h to reservoir c and ρ the particle density inside the reservoirs. The results of the simulations are shown in figure 8(a). The minimum at the reversible limit is clearly visible. Note also that, in contrast to effusion without momentum transfer, the probability distribution behaves smoothly around $\eta = 0$. The explanation is that, due to the possibility of momentum transport alone, small efficiencies arise without net particle transport.

To evaluate the large deviation function of the efficiency, we first note that:

$$
\left\langle e^{-\lambda_W w - \lambda_Q q}\right\rangle = \left\langle e^{-\lambda_W\left(A_N \Delta N + A_{p_x} \Delta p_x\right) - \lambda_q A_U \Delta U}\right\rangle, \tag{35}
$$

and therefore the cumulant generating function of the produced work and heat $\mu_0(\lambda_W, \lambda_Q)$ can be written in terms of the cumulant generating function of the transferred momentum, energy and particle numbers $\mu_1(\lambda_U, \lambda_N, \lambda_{p_x})$:

(a) Schematic representation of the Mandal-Jarzynski model with 3 energy states.

(b) Alternative physical implementation of the Mandal-Jarzynski model.

Figure 9. Possible set-ups for the Mandal–Jarzynski model.

$$\mu_0\left(\lambda_W, \lambda_Q\right) = \mu_1\left(A_N\lambda_W, A_{P_x}\lambda_W, A_U\lambda_Q\right)$$

$$= \sigma\left(\frac{k_B}{2\pi m}\right)^{1/2}\rho T_h^{1/2}\left(1 - \frac{G_h\left(A_N\lambda_W, A_{P_x}\lambda_W, A_U\lambda_Q\right)}{\left(1 + k_B T_h A_U\lambda_Q\right)^2}\right)$$

$$+ \sigma\left(\frac{k_B}{2\pi m}\right)^{1/2}\rho T_c^{1/2}\left(1 - \frac{G_c\left(A_N\lambda_W, A_{P_x}\lambda_W, A_U\lambda_Q\right)}{\left(1 - k_B T_c A_U\lambda_Q\right)^2}\right), \tag{36}$$

with:

$$G_h\left(\lambda_N, \lambda_{P_X}, \lambda_U\right) = \exp\left(-\lambda_N - \frac{mV_h^2\lambda_U - k_B mT_h\lambda_{P_x}^2 + 2mV_h\lambda_{P_x}}{2\left(1 + k_B T_h\lambda_U\right)}\right), \tag{37}$$

and

$$G_c\left(\lambda_N, \lambda_{P_X}, \lambda_U\right) = \exp\left(\lambda_N + \frac{mV_c^2\lambda_U + k_B mT_c\lambda_{P_x}^2 + 2mV_c\lambda_{P_x}}{2\left(1 - k_B T_c\lambda_U\right)}\right). \tag{38}$$
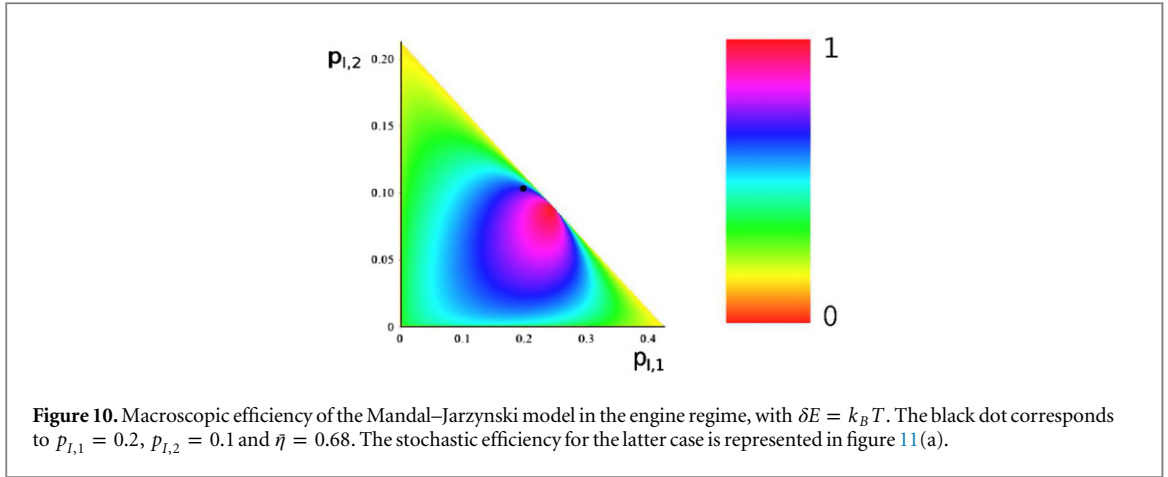
As was discussed for the effusion model, the large deviation can then be found by numerically contracting the cumulant generating function:

$$J\left(\eta\right) = -\min_\lambda \mu_0(\lambda, \lambda\eta) = -\min_\lambda \mu_1\left(A_N\lambda, A_{P_x}\lambda, A_U\eta\lambda\right). \tag{39}$$

The comparison with simulations is shown in figure 8(b). The extrapolation ansatz seems to work quite well apart from an overshoot at the reversible efficiency.

5. Mandal–Jarzynski model

Recently, there has been considerable interest in the stochastic information-to-work conversion. To study this issue in the context of stochastic efficiency, we focus on one of the simplest models, namely the Mandal–Jarzynski engine [10], cf figure 9(a). A particle, in contact with a heat bath at constant temperature *T*, can make transitions between a number of energy levels, which are multiples of δE. Apart from the thermal dissipative transitions due to the bath, the particle undergoes transitions that are driven by the entries of a linear tape. This interaction corresponds to a form of input work. The energy levels of the systems are numbered as shown in figure 9(a). The input tape consists of a sequence of entry values, each referring uniquely to one of the possible energies, which are presented subsequently to the system. During such an interaction, the particle is moved to the energy level with number equal to the initial value on the tape. In this way, work is delivered. After each entry of the tape, the system is left to thermalize, and the new energy state of the particle is written into the tape, which we call the final or exit value. Note that this will alter the Shannon entropy of the tape. The tape moves on one step and the process is repeated. We mention a closely related implementation of the Mandal–Jarzynski model, shown in figure 9(b). A Brownian particle in contact with a thermal bath at temperature *T*, can make jumps on a

Figure 10. Macroscopic efficiency of the Mandal–Jarzynski model in the engine regime, with $\delta E = k_B T$. The black dot corresponds to $p_{I,1} = 0.2$, $p_{I,2} = 0.1$ and $\bar{\eta} = 0.68$. The stochastic efficiency for the latter case is represented in figure 11(a).

discrete lattice with a wall at position zero and a force gradient in the negative direction, inducing an energy difference between two neighbouring sites equal to δE. After the particle has thermalized, its position is measured, and the wall is instantaneously brought to the measured position. Next the wall is adiabatically moved back to the original position with delivery of work, after which the process is repeated. While we studied both versions, we focus in the following on the simplest situation giving nontrivial results for stochastic efficiency, namely a Mandal–Jarzynski model with three states, cf figure 9(a).

It is clear that the amount of delivered work after one entry (trit) of the tape is given by:

$$w = \delta E (f - i), \tag{40}$$

where i and f are the initial and final state of the system, respectively. As is discussed in detail in [8, 18], the Mandal–Jarzynski system operates as an information engine with time-symmetric driving when considering the following definition of the entropy production:

$$\Delta s_{\text{tape}} = k_B \left(\ln \left(p_{I,i} \right) - \ln \left(p_{I,f} \right) \right), \tag{41}$$

with i and f the initial and final state of the trit and $p_{I,k}$ the probability for entry state k on the tape. The average information entropy change upon processing one trit is thus given by:

$$\left\langle \Delta s_{\text{tape}} \right\rangle = k_B \sum_j \left(p_{I,j} - p_{F,j} \right) \ln \left(p_{I,j} \right). \tag{42}$$

Here:

$$p_{F,j} = e^{-j \frac{\delta E}{k_B T}} \Big/ \left(1 + e^{-\frac{\delta E}{k_B T}} + e^{-2\frac{\delta E}{k_B T}} \right), \tag{43}$$

is the probability that the trit leaves the system in state j ($j = 0, 1, 2$). The information entropy written in this way is the sum of the change in Shannon entropy and the entropy production of an auxiliary Mandal–Jarzynski system if it were to bring the tape back to its original distribution [9].
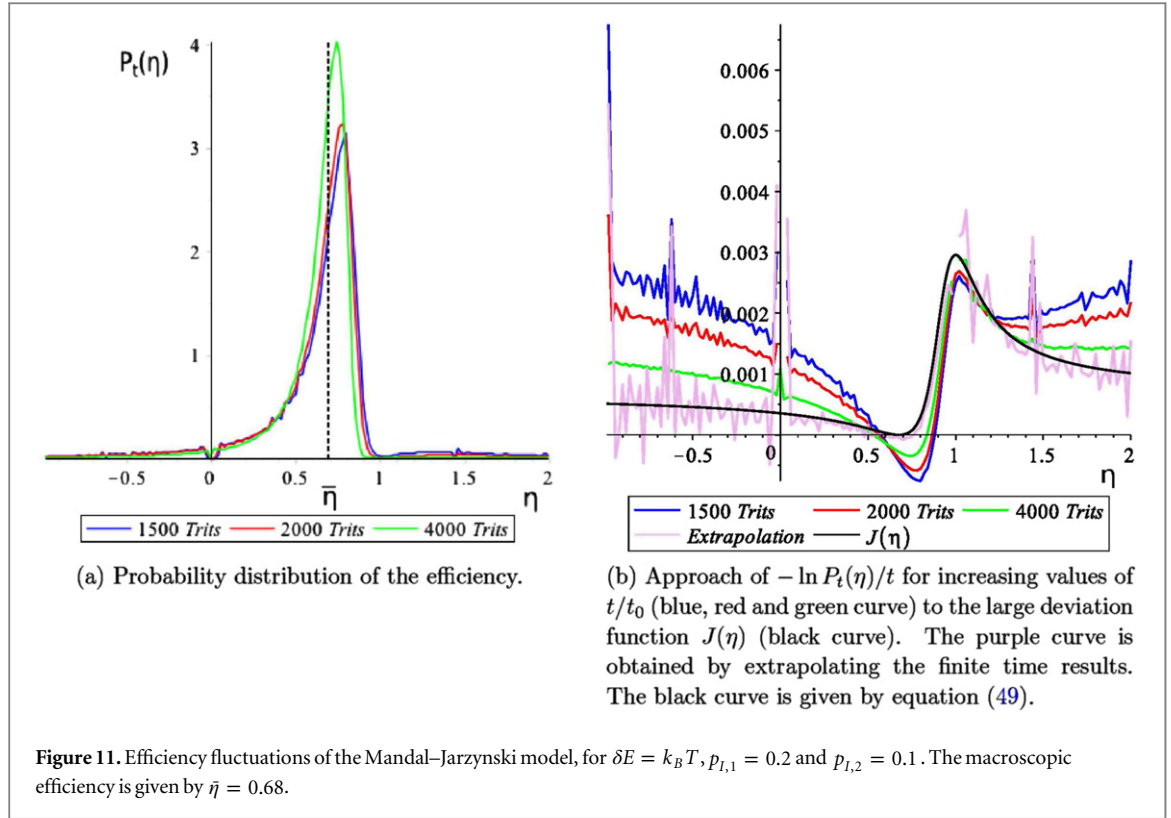
The efficiency is defined as the ratio of the delivered work and the amount of information consumed. In particular the macroscopic efficiency is given by:

$$\bar{\eta} = \frac{\langle w \rangle}{T \left\langle \Delta s_{\text{tape}} \right\rangle}$$

$$= \frac{\delta E}{k_B T} \frac{\left(2\left(p_{F,2} - p_{I,2} \right) + \left(p_{F,1} - p_{I,1} \right) \right)}{\left(\left(p_{I,0} - p_{F,0} \right) \ln \left(p_{I,0} \right) + \left(p_{I,1} - p_{F,1} \right) \ln \left(p_{I,1} \right) + \left(p_{I,2} - p_{F,2} \right) \ln \left(p_{I,2} \right) \right)}. \tag{44}$$

A colour-coded plot is given in figure 10, for $\delta E / k_B T = 1$. Reversible efficiency ($\bar{\eta} = 1$) can be reached in the limit where $p_{I,j} = p_{F,j}, j = 1, 2$, with $p_{I,1} - p_{F,1} \neq 2(p_{F,2} - p_{I,2})$, cf figure 10.

The joint probability distribution $P_{\text{init},N}(n_1, n_2)$ of n_1 and n_2 incoming trits with value 1 and 2 respectively on a total of N trits is given by:

$$P_{\text{init},N}(n_1, n_2) = \frac{N!}{(N - n_1 - n_2)! n_1! n_2!} p_{I,1}^{n_1} p_{I,2}^{n_2} \left(1 - p_{I,1} - p_{I,2} \right)^{N - n_1 - n_2} \tag{45}$$

(a) Probability distribution of the efficiency.

(b) Approach of $-\ln P_t(\eta)/t$ for increasing values of t/t_0 (blue, red and green curve) to the large deviation function $J(\eta)$ (black curve). The purple curve is obtained by extrapolating the finite time results. The black curve is given by equation (49).

Figure 11. Efficiency fluctuations of the Mandal–Jarzynski model, for $\delta E = k_B T$, $p_{I,1} = 0.2$ and $p_{I,2} = 0.1$. The macroscopic efficiency is given by $\bar{\eta} = 0.68$.

and the joint probability distribution of n_1 and n_2 outgoing trits with value 1 and 2 respectively on a total of N trits is given by:

$$P_{\text{Final},N}(n_1, n_2) = \frac{N!}{(N - n_1 - n_2)!\,n_1!\,n_2!} p_{F,1}^{n_1} p_{F,2}^{n_2} \left(1 - p_{F,1} - p_{F,2}\right)^{N - n_1 - n_2}, \tag{46}$$

which is independent of the distribution of the incoming trits. Using these distributions, numerical simulations can be performed, to evaluate the probability distribution of the stochastic efficiency

$$\eta = \frac{w}{T \Delta s_{\text{tape}}}, \tag{47}$$

cf figure 11(a). The minimum around $\eta = 0$ is analogous to the minimum in the effusion model, and disappears in the large time limit. Furthermore, one observes the weak local minimum at reversible efficiency one with, to its right, a more clearly visible maximum.

The large deviation functions of $x_1 = n_{I,1}/N$ and $x_2 = n_{I,2}/N$ incoming trits with value 1 and 2 respectively, is found from equation (45):

$$\gamma_{\text{Init}}(x_1, x_2) = x_1 \ln(x_1) + x_2 \ln(x_2) + (1 - x_1 - x_2)\ln(1 - x_1 - x_2)$$
$$- x_1 \ln(p_{I,1}) - x_2 \ln(p_{I,2}) - (1 - x_1 - x_2)\ln(1 - p_{I,1} - p_{I,2}), \tag{48}$$

and a completely analogous expression for the large deviation function $\gamma_{\text{Final}}(y_1, y_2)$ of $y_1 = n_{F,1}/N$ and $y_2 = n_{F,2}/N$, with $p_{I,k}$ replaced by $p_{F,k}$. From this, the large deviation function of the efficiency can be calculated:

$$J(\eta) = \min_{x_1, x_2, y_1, y_2} \left(\gamma_{\text{Init}}(x_1, x_2) + \gamma_{\text{Final}}(y_1, y_2)\right), \tag{49}$$

where x_1, x_2, y_1 and y_2 are constrained to reproduce the efficiency η under consideration, i.e., they are related by:

$$\eta = \frac{\delta E}{k_B T} \frac{\left(2(y_2 - x_2) + y_1 - x_1\right)}{(x_0 - y_0) \ln\left(p_{I,0}\right) + (x_1 - y_1) \ln\left(p_{I,1}\right) + (x_2 - y_2) \ln\left(p_{I,2}\right)}. \tag{50}$$

This minimisation can be done numerically, cf figure 11(b). In spite of the noise, which is mainly due to the discreteness of the efficiency, the extrapolation seems to work quite well. Also, the telltale maximum in the large deviation function close to reversible efficiency is again reproduced.

6. Discussion

The concept of efficiency plays a crucial role in thermodynamics, especially when the efficiency is defined in such a way that is leads to universal system-independent statements, such as the one concerning Carnot efficiency. With the advent of stochastic thermodynamics, it is natural to revisit such questions for stochastic efficiency. Universal statements appear to be possible for the large deviation function characterizing the asymptotic time regime. In particular, long-time realisations with reversible efficiency are exponentially least probable for time-symmetric driving. One purpose of this paper has been to verify and document the salient features of the time-asymptotic stochastic efficiency in five different settings, namely driven Brownian motion, effusion with a thermo-chemical and thermo-velocity gradient, a quantum dot and a model for information to work conversion. In addition, we provide the analysis for finite time including the approach to and extrapolation into the asymptotic time regime. A revealing feature of our analysis is that the large deviation properties can be obtained quite consistently by extrapolation from rather short finite time results. The other encouraging message is that one can apply the analysis to a wide variety of completely different implementations, some of which may be easier to realize. Both observations imply that an experimental verification should not pose a real problem. In particular, in view of existing experiments on the issue [21, 23, 50–52], the experimental implementation for the stochastic efficiency of an information to work engine should be relatively straigthforward.

Acknowledgments

Appendix A. Large deviation functions from finite time results

The central object of interest in stochastic efficiency is its large deviation function. Unfortunately, the evaluation of exponentially unlikely events is obviously very difficult. For this reason, we propose a simple and apparently robust method to deduce the large deviation function $J(\eta)$ from finite time results. As input we give the efficiency probability distributions for three finite times t_1, t_2 and t_3. We propose the following ansatz for $P_t(\eta)$:

$$P_{\text{Fit},t}(\eta) = A(\eta) t^{-B(\eta)} e^{-tJ(\eta)}. \tag{A.1}$$

Here, $A(\eta)$, $B(\eta)$ and $J(\eta)$ are three fitting parameters for each η. $J(\eta)$ shall be our estimate for the large deviation function. The fitting parameters can be obtained from the known values $-\ln(P_{t_i}(\eta))$, with $i = 1, 2, 3$, since:

$$\begin{bmatrix} -\ln\left(P_{t_1}(\eta)\right)/t_1 \\ -\ln\left(P_{t_2}(\eta)\right)/t_2 \\ -\ln\left(P_{t_3}(\eta)\right)/t_3 \end{bmatrix} = \begin{bmatrix} 1 & 1/t_1 & \ln(t_1)/t_1 \\ 1 & 1/t_2 & \ln(t_2)/t_2 \\ 1 & 1/t_3 & \ln(t_3)/t_3 \end{bmatrix} \begin{bmatrix} J(\eta) \\ -\ln(A(\eta)) \\ B(\eta) \end{bmatrix}. \tag{A.2}$$

Inverting this matrix equality leads to an estimate of the large deviation function.

Appendix B. Efficiency calculations from event probability distributions

Consider a model consisting of k tight-coupled processes (e.g. k channels for particle transport), where the ith process undergoes n_i events, $i = 1,..,k$. Furthermore, the total delivered amount of work and heat can be written as $W(n_1, \ldots, n_k)$ and $Q(n_1, \ldots, n_k)$. Once the event probability distribution is known, the probability distribution of η can be written as:

$$P_t(\eta) = \sum_{n_1,\ldots,n_k} P_t(n_1, \ldots, n_k) \delta_{\eta Q(n_1,\ldots,n_k), W(n_1,\ldots,n_k)}, \tag{B.1}$$

for discrete variables and

$$P_t(\eta) = \int dn_1 .. dn_k P_t(n_1, \ldots, n_k) \delta\left(\eta - \frac{W(n_1, \ldots, n_k)}{Q(n_1, \ldots, n_k)}\right), \tag{B.2}$$

for continuous variables, where $P_t(n_1, \ldots, n_k)$ is the probability that at time t, for process i, n_i events have occured. Using the corresponding event large deviation function

$\gamma\left(n_1, \ldots, n_k\right) = -\lim_{t\to\infty}\left(1/t \, \ln\left(P_t\left(n_1, \ldots, n_k\right)\right)\right)$, the efficiency large deviation function $J(\eta)$ can then be calculated via the contraction principle:

$$J(\eta) = \min_{n_1, \ldots, n_k} \gamma\left(n_1, \ldots, n_k\right), \tag{B.3}$$

where $n_1, \ldots, n_k$ are conditioned to:

$$\eta = \frac{W\left(n_1, \ldots, n_k\right)}{Q\left(n_1, \ldots, n_k\right)}. \tag{B.4}$$

This provides a good scheme for numerical calculations.

We proceed to show that there are, in this case, only two extrema of the efficiency large deviation function: the macroscopic efficiency and the reversible efficiency. Using Lagrange multipliers, we have:

$$J(\eta) = \text{Extr}_{x_1, \ldots, x_k, \lambda} L\left(x_1, \ldots, x_k, \lambda\right), \tag{B.5}$$

with

$$L\left(x_1, \ldots, x_k, \lambda\right) = \gamma\left(x_1, \ldots, x_k\right) + \lambda\left(\eta Q\left(x_1, \ldots, x_k\right) - W\left(x_1, \ldots, x_k\right)\right). \tag{B.6}$$

Therefore, $x_1, \ldots, x_k, \lambda$ are constrained to:

$$\frac{\partial\gamma\left(x_1, \ldots, x_k\right)}{\partial x_i} = -\lambda\left(\eta\frac{\partial Q\left(x_1, \ldots, x_k\right)}{\partial x_i} - \frac{W\left(x_1, \ldots, x_k\right)}{\partial x_i}\right), \tag{B.7}$$

for all i. As $L\left(x_1, \ldots, x_k, \lambda\right)$ is an extremum of λ and $x_i, i = 1, \ldots, k$, we have

$$\begin{aligned}
\frac{\mathrm{d}}{\mathrm{d}\eta}J(\eta) &= \sum_i \frac{\partial L\left(x_1, \ldots, x_k, \lambda\right)}{\partial x_i}\frac{\partial x_i}{\partial\eta} + \frac{\partial L\left(x_1, \ldots, x_k, \lambda\right)}{\partial\lambda}\frac{\partial\lambda}{\partial\eta} + \frac{\partial L\left(x_1, \ldots, x_k, \lambda\right)}{\partial\eta} \\
&= \frac{\partial L\left(x_1, \ldots, x_k, \lambda\right)}{\partial\eta} \\
&= \lambda Q\left(x_1, \ldots, x_k\right).
\end{aligned} \tag{B.8}$$

Note that $Q\left(x_1, \ldots, x_k\right) = 0$ corresponds to reversible efficiency due to the fluctuation theorem, and that $\lambda = 0$ corresponds to $\partial\gamma\left(x_1, \ldots, x_k\right)/\partial x_i = 0$ (using equation (B.7)) which is equivalent with macroscopic efficiency (as we assume convex event large deviation functions). As one of these two equalities has to be fulfilled to be in an extremum of $J(\eta)$, we conclude that these are the only two extremums of the large deviation function.

We finally note that the expression for $J(\eta)$ can be further simplified if the processes are independent. We shall illustrate this for systems consisting of two independent processes (with n_1 and n_2 events respectively). The extension to more independent processes is straightforward. The amount of delivered work per event in the ith process is written as w_i and the amount of extracted heat is $q_i, i = 1, 2$. The efficiency is then given by:

$$\begin{aligned}
\eta &= \frac{w_1 n_1 + w_2 n_2}{q_1 n_1 + q_2 n_2} \\
&= \frac{q_1 n_1}{q_1 n_1 + q_2 n_2}\eta_1 + n_2\frac{q_2 n_2}{q_1 n_1 + q_2 n_2}\eta_2 \\
&= \alpha\eta_1 + (1-\alpha)\eta_2,
\end{aligned} \tag{B.9}$$

with

$$\alpha = \frac{q_1 n_1}{q_1 n_1 + q_2 n_2} = \frac{\eta - \eta_2}{\eta_1 - \eta_2}, \tag{B.10}$$

and $\eta_i = w_i/q_i, i = 1, 2$. Therefore, the probability distribution of η at time t is given by:

$$\begin{aligned}
P_t(\eta) &= \int\int \mathrm{d}w\mathrm{d}q P_t(w, q)\delta\left(\eta - \frac{w}{q}\right) \\
&= \int\int \mathrm{d}n_1\mathrm{d}n_2 \left|w_1 q_2 - w_2 q_1\right| P_t\left(n_1\right)P_t\left(n_2\right)\delta\left(\eta - \alpha\eta_1 - (1-\alpha)\eta_2\right).
\end{aligned} \tag{B.11}$$

From large deviation theory, we can now write the efficiency large deviation function $J(\eta)$ in terms of terms of the large deviation functions of the event numbers $\varphi_1\left(n_1\right)$ and $\varphi_2\left(n_2\right)$:

$$J(\eta) = \min_x\left(\varphi_1\left(\frac{\alpha x}{q_1}\right) + \varphi_2\left(\frac{(1-\alpha)x}{q_2}\right)\right). \tag{B.12}$$

Appendix C. Event large deviation function of quantum dot-like models

We present for completeness the large deviation function for the number of particles travelling through one energy level of a quantum dot (with energy E and coupling constant $\Gamma = 1$). We only quote the final result, as similar calculations can be found in the literature, see e.g. [53–56]. We recall that the fluxes are given by equations (18) and (19). The cumulant generating function is given by:

$$f(\gamma) = k + \sqrt{r + q(\gamma)s}, \tag{C.1}$$

with

$$k = -\frac{\left(k_L^+ + k_L^- + k_R^+ + k_R^-\right)}{2}; \quad s = \sqrt{k_L^+ k_R^+ k_L^- k_R^-}; \quad \gamma_0 = \ln\left(\frac{k_L^+ k_R^-}{k_R^+ k_L^-}\right)$$

$$\rho(\gamma) = e^{\gamma_0/2 - \gamma}; \quad r = k^2 - k_L^+ k_R^- - k_R^+ k_L^-; \quad q(\gamma) = \rho(\gamma) + \rho(\gamma)^{-1}. \tag{C.2}$$

The large deviation function reads:

$$h(n) = -f(\gamma(n)) - n\gamma(n), \tag{C.3}$$

with:

$$\bar{q}(n) = \frac{2n}{s}\sqrt{r + 2n^2 + 2\sqrt{s^2 + rn^2 + n^4}}, \tag{C.4}$$

$$\gamma(n) = \frac{\gamma_0}{2} - \ln\left(\frac{\sqrt{\bar{q}(n)^2 + 4} + \bar{q}(n)}{2}\right). \tag{C.5}$$

References

[1] Szilard L 1929 *Z. Phys.* **53** 840–56
[2] Leff H and Rew A 2002 *Maxwell's Demon 2 Entropy, Classical and Quantum Information, Computing* (Boca Raton, FL: CRC Press)
[3] Parrondo J M and Español P 1996 *Am. J. Phys.* **64** 1125–9
[4] Sekimoto K 1997 *J. Phys. Soc. Japan* **66** 1234–7
[5] Jarzynski C and Mazonka O 1999 *Phys. Rev.* E **59** 6448
[6] Van den Broeck C, Kawai R and Meurs P 2004 *Phys. Rev. Lett.* **93** 090601
[7] Sekimoto K 1998 *Prog. Theor. Phys. Suppl.* **130** 17–27
[8] Barato A and Seifert U 2014 *Phys. Rev. Lett.* **112** 090601
[9] Barato A and Seifert U 2014 *Phys. Rev.* E **90** 042150
[10] Mandal D and Jarzynski C 2012 *Proc. Natl Acad. Sci. USA* **109** 11641–5
[11] Touchette H and Lloyd S 2000 *Phys. Rev. Lett.* **84** 1156
[12] Sagawa T and Ueda M 2010 *Phys. Rev. Lett.* **104** 090602
[13] Horowitz J M and Parrondo J M 2011 *New J. Phys.* **13** 123019
[14] Kish L B and Granqvist C G 2012 *Europhys. Lett.* **98** 68001
[15] Abreu D and Seifert U 2012 *Phys. Rev. Lett.* **108** 030601
[16] Mandal D, Quan H and Jarzynski C 2013 *Phys. Rev. Lett.* **111** 030602
[17] Esposito M and Schaller G 2012 *Europhys. Lett.* **99** 30003
[18] Horowitz J M, Sagawa T and Parrondo J M 2013 *Phys. Rev. Lett.* **111** 010602
[19] Raizen M G 2009 *Science* **324** 1403–6
[20] Raizen M G 2011 *Sci. Am.* **304** 54–59
[21] Bérut A, Arakelyan A, Petrosyan A, Ciliberto S, Dillenschneider R and Lutz E 2012 *Nature* **483** 187–9
[22] Thorn J J, Schoene E A, Li T and Steck D A 2008 *Phys. Rev. Lett.* **100** 240407
[23] Toyabe S, Sagawa T, Ueda M, Muneyuki E and Sano M 2010 *Nat. Phys.* **6** 988–92
[24] Strasberg P, Schaller G, Brandes T and Esposito M 2013 *Phys. Rev. Lett.* **110** 040601
[25] Serreli V, Lee C F, Kay E R and Leigh D A 2007 *Nature* **445** 523–7
[26] Jarzynski C 1997 *Phys. Rev. Lett.* **78** 2690
[27] Crooks G E 1999 *Phys. Rev.* E **60** 2721
[28] Seifert U 2012 *Rep. Prog. Phys.* **75** 126001
[29] van den Broeck C and Esposito M 2015 *Physica* A **418** 6–16
[30] Becker T, Willaert T, Cleuren B and van den Broeck C 2015 *Phys. Rev.* E **91** 012101
[31] Evans D J, Cohen E and Morriss G 1993 *Phys. Rev. Lett.* **71** 2401
[32] Gallavotti G and Cohen E G D 1995 *Phys. Rev. Lett.* **74** 2694
[33] Lebowitz J and Spohn H 1999 *J. Stat. Phys.* **95** 333
[34] Kurchan J 1998 *J. Phys. A: Math. Gen.* **31** 3719
[35] Verley G, Willaert T, van den Broeck C and Esposito M 2014 *Nat. Commun.* **5** 4721
[36] Gingrich T R, Rotskoff G M, Vaikuntanathan S and Geissler P L 2014 *New J. Phys.* **16** 102003
[37] Verley G, Willaert T, van den Broeck C and Esposito M 2014 *Phys. Rev.* E **90** 052145
[38] Proesmans K, Cleuren B and van den Broeck C 2015 *Europhys. Lett.* **109** 20004
[39] Polettini M, Verley G and Esposito M 2015 *Phys. Rev. Lett.* **114** 050601
[40] Rana S, Pal P, Saha A and Jayannavar A 2014 *Phys. Rev.* E **90** 042146

[41] Campisi M, Pekola J and Fazio R 2014 *New J. Phys.* **17** 035012
[42] Esposito M, Ochoa M A and Galperin M 2015 *Phys. Rev. B* **91** 115417
[43] Martinez I A, Roldan E, Dinis L, Petrov D, Parrondo J M and Rica R 2014 arXiv: 1412.1282
[44] Cleuren B, van den Broeck C and Kawai R 2006 *Phys. Rev. E* **74** 021117
[45] Esposito M, Lindenberg K and van den Broeck C 2009 *Europhys. Lett.* **85** 60010
[46] Esposito M, Kawai R, Lindenberg K and van den Broeck C 2010 *Europhys. Lett.* **89** 20003
[47] Esposito M, Kawai R, Lindenberg K and van den Broeck C 2010 *Phys. Rev. E* **81** 041106
[48] Esposito M, Kumar N, Lindenberg K and van den Broeck C 2012 *Phys. Rev. E* **85** 031117
[49] Wood K, van den Broeck C, Kawai R and Lindenberg K 2007 *Phys. Rev. E* **75** 061116
[50] Wang G M, Sevick E M, Mittag E, Searles D J and Evans D J 2002 *Phys. Rev. Lett.* **89** 050601
[51] Blickle V, Speck T, Helden L, Seifert U and Bechinger C 2006 *Phys. Rev. Lett.* **96** 070603
[52] Gieseler J, Quidant R, Dellago C and Novotny L 2014 *Nat. Nanotechnology* **9** 358–64
[53] Willaert T, Cleuren B and van den Broeck C 2014 *Eur. Phys. J. B* **87** 1–4
[54] Lacoste D, Lau A and Mallick K 2008 *Phys. Rev. E* **78** 011915
[55] Harris R and Schütz G 2007 *J. Stat. Mech. Theory Exp.* **2007** P07020
[56] Verley G, van den Broeck C and Esposito M 2013 *Phys. Rev. E* **88** 032137